Bone Reports 12 (2020) 100260

Contents lists available at ScienceDirect

Bone Reports

journal homepage: www.elsevier.com/locate/bonr

Theoretical concept of cortical to cancellous bone transformation

Yoshitaka Kameo[a,b,c,*], Nobuaki Sakano[b], Taiji Adachi[a,b,c]

[a] Department of Biosystems Science, Institute for Frontier Life and Medical Sciences, Kyoto University, Japan
[b] Department of Micro Engineering, Graduate School of Engineering, Kyoto University, Japan
[c] Department of Mammalian Regulatory Network, Graduate School of Biostudies, Kyoto University, Japan

ARTICLE INFO

Keywords:
Cortical bone
Cancellous bone
Cortical-to-cancellous bone transformation
Remodeling simulation
Mathematical model

ABSTRACT

Microstructures of cortical and cancellous bones are altered continually by load-adaptive remodeling; in addition, their cellular mechanisms are similar despite the remarkably different porosities. The cortico-cancellous transitional zone is a site of vigorous remodeling, and intracortical remodeling cavitates the inner cortex to promote its trabecularization, which is considered the main cause of bone loss because of aging. Therefore, to prevent and treat age-related cortical bone loss effectively, it is indispensable to gain an integrated understanding of the cortical to the cancellous bone transformation via remodeling. We propose a novel theoretical concept to account for the transformation of dense cortical bone to porous cancellous bone. We develop a mathematical model of cortical and cancellous bone remodeling based on the concept that bone porosity is determined by the balance between the load-bearing function of mineralized bone and the material-transporting function of bone marrow. Remodeling simulations using this mathematical model enable the reproduction of the microstructures of cortical and cancellous bones simultaneously. Furthermore, current remodeling simulations have the potential to replicate cortical-to-cancellous bone transformation based on changes in the local balance between bone formation and resorption. We anticipate that the proposed mathematical model of cortical and cancellous bone remodeling will contribute to highlighting the essential features of cortical bone loss due to trabecularization of the cortex and help predict its spatial and temporal behavior during aging.

1. Introduction

Adult bones can be classified into two distinct types based on their porosities: cortical and cancellous bones. The microstructures of these bones are altered by load-adaptive remodeling to satisfy mechanical demands. Consequently, osteons in dense cortical bone and trabeculae in porous cancellous bone are aligned along the direction of local loading (Petrtyl et al., 1996; Wolff, 1870, 2010). Cellular mechanisms of cortical and cancellous bone remodeling are similar despite their remarkable difference in porosity; bone remodeling is performed by basic multicellular units that comprise bone-resorbing osteoclasts and bone-forming osteoblasts (Parfitt, 1994), and these effector cells activities are believed to be orchestrated by osteocytes buried in the mineralized bone matrix (Bonewald, 2011). Bone porosity can vary continuously from the cortical to the cancellous bone (Zebaze et al., 2013); this cortico-cancellous transitional zone is a site of vigorous remodeling, and intracortical remodeling that occurs on the surface of Haversian and Volkmann canals cavitates the inner cortex to promote its trabecularization, which is considered the main cause of bone loss because of aging (Bala et al., 2015; Zebaze et al., 2010). Therefore, to prevent and treat age-related cortical bone loss effectively, it is indispensable to gain an integrated understanding of the transformation from the cortical to the cancellous bone by remodeling.

Computer simulations using mathematical models of bone remodeling have contributed to investigations of changes in bone microstructure in response to mechanical loadings (Gerhard et al., 2009). Although they could reproduce the load-adaptive orientation of osteons in the cortical bone (van Oers et al., 2008) and trabeculae in the cancellous bone (Badilatti et al., 2016; Huiskes et al., 2000; Kameo and Adachi, 2014) successfully, the transformation between the two types of bone has not been addressed and the understanding relating to its mechanism remains limited. Most previous mathematical models focused on the change in mineralized bone volume because it is responsible for the load-bearing function. However, bone marrow within nonmineralized space plays an important role in bone remodeling by providing a microenvironment to nurture mesenchymal and hematopoietic stem cells from which osteoblasts and osteoclasts are derived, respectively (Mendez-Ferrer et al., 2010), and to transport oxygen,

* Corresponding author at: Department of Biosystems Science, Institute for Frontier Life and Medical Sciences, Kyoto University, 53 Kawahara-cho, Shogoin, Sakyo-ku, Kyoto 606-8507, Japan.
E-mail address: kameo@infront.kyoto-u.ac.jp (Y. Kameo).

https://doi.org/10.1016/j.bonr.2020.100260
Received 5 December 2019; Received in revised form 2 March 2020; Accepted 19 March 2020
Available online 24 March 2020

nutrients, hormones, and other signaling molecules from blood vessels to various cells (Ramasamy, 2017). To understand the mechanism of cortical-to-cancellous bone transformation through computer simulations, which can be determined explicitly from an increase in the volume ratio of the bone marrow to the mineralized bone, it is necessary to consider the effects of bone marrow in the mathematical model for bone remodeling simulations.

We propose a novel theoretical concept to account for the transformation of dense cortical bone to porous cancellous bone for reproducing and predicting age-related cortical bone loss accompanied by the trabecularization of the cortex. We develop a mathematical model of cortical and cancellous bone remodeling based on the theoretical concept that bone porosity is determined by the balance between the load-bearing function of mineralized bone and the material-transporting function of bone marrow. Considering that the change in bone morphology due to bone formation and resorption can be described by the movement of the interface between the mineralized bone and bone marrow, we assume that bone formation is promoted by mechanical stress experienced by the mineralized bone, whereas bone resorption is caused by molecules supplied by blood vessels, which diffuse within bone marrow space. To show the potential abilities of the proposed remodeling model, we investigated the dependence of model parameters associated with mechanical stress and concentration of bone resorption molecules on the microstructures of cortical-like and cancellous-like bones through the replication of cortical-to-cancellous bone transformation.

2. Methods

2.1. Mathematical model of bone remodeling

The difference in the porosities of the cortical and cancellous bones is considered to result from the difference in the local balance between bone formation and resorption. On the one hand, bone formation, *i.e.*, the increase in mineralized bone volume, is associated with the improvement of the load-bearing function of mineralized bone. On the other hand, bone resorption, *i.e.*, the increase in bone marrow volume, is associated with the improvement of the material-transport function of bone marrow. The equilibrium state of bone remodeling can be achieved when these two functions are balanced locally. Accordingly, we propose a mathematical model of bone remodeling based on the assumption that bone formation is induced by the mechanical factor in mineralized bone, and bone resorption is induced by the biochemical factor in the bone marrow, as shown in Fig. 1a.

Bone remodeling is considered to be regulated mechanically by osteocytes, which are regarded as major mechanosensory cells (Bonewald, 2011). Osteocytes produce sclerostin—a protein known to be a potent inhibitor of bone formation—the expression of which is reduced by mechanical loading (Robling et al., 2008; Spatz et al., 2015). Although osteocytes are believed to be stimulated by interstitial fluid flow (Weinbaum et al., 1994), for the sake of simplicity, we assume that osteocytes are susceptible to von Mises equivalent stress of the surrounding bone matrix σ_{eq} because it is a representative scalar variable that is positively correlated with flow velocity. Considering that the flow stimulus to the osteocytes is dominant in the neighborhood of the bone surface (Kameo et al., 2009, 2016), in our modeling, we introduced the mechanical stimulus S_{sf} that drives bone formation on the bone surface $\boldsymbol{x}_{sf}$ as a weighted average of σ_{eq} on the bone surface (Kim et al., 2017):

$$S_{sf}(\boldsymbol{x}_{sf}) = \frac{\int_A w(l)\sigma_{eq}(\boldsymbol{x})dA}{\int_A w(l)dA} \tag{1}$$

where A is the bone surface domain, and $w(l)$ denotes a weight function that decays with distance $l = |\boldsymbol{x}_{sf} - \boldsymbol{x}|$ and takes a nonzero value only when l is smaller than the sensing distance l_L.

Bone remodeling is also regulated by various signaling molecules that are transported throughout the bone marrow space. In contrast to mechanical stimulus as a bone formation factor, we considered a hypothetical molecule, provided by blood vessels, that works as a bone resorption factor. The parathyroid hormone (PTH) is one such candidate molecule because continuous exposure to PTH stimulates bone resorption (Silva and Bilezikian, 2015). The concentration of the molecule, ϕ, in the bone marrow space varies according to the following diffusion equation:

$$\frac{\partial \phi}{\partial t} = D\nabla^2\phi - k\phi \tag{2}$$

where D is the diffusion coefficient and k is the degradation rate constant. The molecular concentration on the bone surface $\boldsymbol{x}_{sf}$ was assumed to influence bone resorption. By introducing the dimensionless values

$$\bar{\boldsymbol{x}} = \frac{\boldsymbol{x}}{L}, \quad \bar{t} = \frac{Dt}{L^2}, \quad \bar{\phi} = \frac{\phi}{\phi_0}, \quad \bar{k} = \frac{L^2 k}{D} \tag{3}$$

Eq. (2) can be rewritten in a dimensionless form as

$$\frac{\partial \bar{\phi}}{\partial \bar{t}} = \bar{\nabla}^2\bar{\phi} - \bar{k}\bar{\phi} \tag{4}$$

where L is the representative length, ϕ_0 is the representative concentration, and $\bar{\nabla}^2$ denotes the Laplacian with respect to $\bar{\boldsymbol{x}}$.

Bone remodeling is a cyclical process of bone erosion and deposition, and their relative difference results in the local movement of bone surface. To represent the net changes in mineralized bone morphology caused by repetitive bone resorption and formation, the rate of bone surface movement in the normal outward direction $\dot{M}$, defined in the time scale much longer than that of remodeling cycle, was introduced. The value of $\dot{M}$ was set based on the stages of bone remodeling as

$$\dot{M} = \begin{cases} \dot{M}_{max} & \text{when bone formation} \\ -\dot{M}_{max} & \text{when bone resorption} \\ 0 & \text{when quiescence} \end{cases} \tag{5}$$

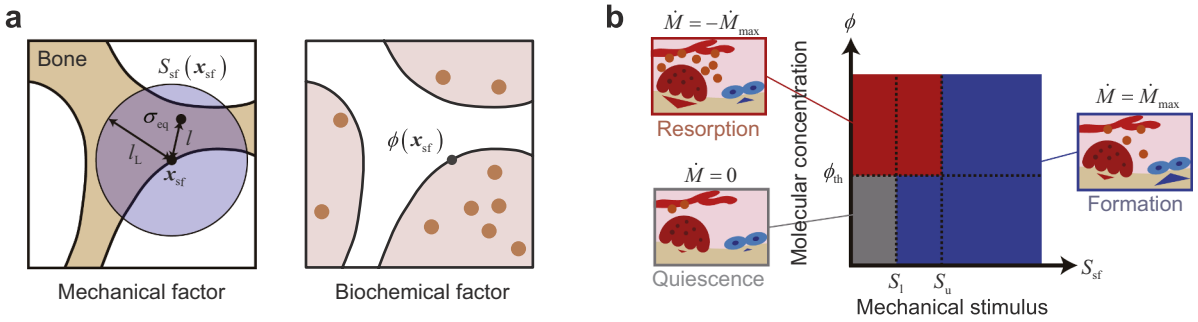

Fig. 1. Mathematical model of bone remodeling based on the assumption that bone formation is induced by a mechanical factor in mineralized bone and bone resorption is induced by a biochemical factor in the bone marrow. a, Mechanical stimulus S_{sf} for bone formation and molecular concentration ϕ for bone resorption. b, Stages of bone remodeling defined by the mechanical stimulus S_{sf} and the molecular concentration ϕ.

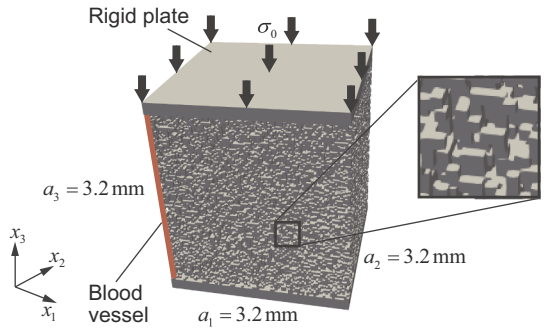

Fig. 2. A voxel finite element model of a cancellous-like bone specimen subjected to uniaxial compressive loading. A single blood vessel was placed at the corner of the region of analysis, from which bone resorption molecules are secreted and diffuse in the marrow space surrounding the mineralized bone.

where $\dot{M}_{max}(>0)$ is the maximum rate of bone surface movement; the stages of bone remodeling were assumed to be determined by the mechanical stimulus S_{sf} and molecular concentration ϕ on the bone surface, as shown in Fig. 1b. When the bone resorption molecules are sufficiently supplied from the blood vessels to the bone surface ($\phi \geq \phi_{th}$), both bone formation and resorption can occur; further, bone is formed when $S_{sf} \geq S_u$ and resorbed when $S_{sf} < S_u$. Conversely, in the case the molecular concentration is relatively low ($\phi < \phi_{th}$), only bone formation occurs when $S_{sf} \geq S_l$ and bone remodeling is under a quiescent state when $S_{sf} < S_l$. In the above modeling, S_u and S_l denote the upper and lower threshold values for the mechanical stimulus S_{sf}, and ϕ_{th} denotes the threshold value for molecular concentration ϕ.

2.2. Voxel-based simulation

We combined the proposed remodeling model with a voxel-based simulation. Mechanical stress in mineralized bone tissue was numerically computed by a voxel finite element method (FEM) (Adachi et al., 2001; Tsubota and Adachi, 2004). A voxel FE model of a cancellous-like bone specimen as an initial simulation model was considered, as shown in Fig. 2. The region of analysis was set to $a_1 \times a_2 \times a_3 = 3.2 \times 3.2 \times 3.2$ mm^3 and discretized by cubic voxel finite elements, with an edge size of 40 μm. To construct an isotropic porous bone structure, many pieces of torus-like bone, with an outer diameter of 0.36 mm and inner diameter of 0.28 mm, were scattered randomly in the entire region; this produced a bone volume fraction (BV/TV) of 0.33. A domain outside the mineralized bone was regarded as the bone marrow space. Two rigid plates were placed on the top and bottom surfaces of the region to apply external loadings. The mineralized bone was assumed to be a homogeneous and isotropic elastic material, with Young's modulus $E = 20$ GPa and Poisson's ratio $\nu = 0.3$.

A single blood vessel along the x_3-direction was set at the corner of the region of analysis, as shown in Fig. 2. In the blood vessel, the concentration of bone resorption molecules was assumed to have a constant value ϕ_0. The diffusion equation (Eqs. (2) or (4)) governing the spatial and temporal behavior of the molecules in the bone marrow space was solved by an explicit finite difference method, where the same voxel mesh as the FEM was used. The parameters for the diffusion analysis were set as $D = 5.0$ μm^2/s and $k = 4.9 \times 10^{-6}$ s^{-1}, which satisfies $\bar{k} = 10$ by setting $L = 3.2$ mm. The order of D was estimated by using the Stokes–Einstein equation, which yields the diffusion coefficient of spherical particles through a fluid with a low Reynolds number. The distribution of molecular concentration in a steady state was used to determine bone formation/resorption on the bone surface.

As mechanical boundary conditions, a uniform uniaxial compressive load $\sigma_0 = -1.0$ MPa was applied on the upper surface of the top plate in the x_3-direction, while keeping the out-of-plane displacement of the lower surface of the bottom plate constrained. The sensing distance l_L to derive the mechanical stimulus S_{sf} was set to $l_L = 200$ μm by referencing the distance of calcium propagation between bone cells (Adachi et al., 2009). In the framework of voxel modeling, the changes in bone morphology can be expressed by the removal/addition of the voxel elements from/to the bone surface. Thus, we set $\dot{M}_{max} = 40$ μm/day (Jaworski and Lok, 1972) by considering the voxel size of the present FE model. To investigate the effects of three model parameters included in the proposed remodeling model, *i.e.*, S_u, S_l, and ϕ_{th}, on the cortical-like and cancellous-like bone microstructures as a result of load-adaptive bone remodeling, we determined the baseline parameter setting as $S_u/\sigma_0 = 4.0$, $S_l/\sigma_0 = 2.0$, and $\phi_{th}/\phi_0 = 1.0 \times 10^{-2}$, and we varied one of these parameters while keeping the other two parameters fixed.

3. Results

3.1. Reproduction of cortical and cancellous bone microstructures

We simulated the bone remodeling of a cubic bone specimen under the baseline parameter setting of S_u, S_l, and ϕ_{th} for 100 days, which corresponds roughly to the time scale of human bone loss due to unloading, such as in space flight and bed rest (LeBlanc et al., 2007). Fig. 3 shows the adaptive change in the bone specimen subjected to uniaxial loading. The color contour indicates von Mises equivalent stress to define the mechanical stimulus S_{sf} for bone formation.

For the first 10 days, the mineralized bone was remarkably eroded, and the marrow space was enlarged in the neighborhood of the blood vessel because the concentration of bone resorption molecules was locally high. Meanwhile, bone deposition in the region far from the blood vessel proceeded because of excess loading, which increased local BV/TV. As a result of the 10-day remodeling, large equivalent stress was produced on the surface of the dense bone that faces the marrow cavity close to the blood vessel. During the period from 10 to 30 days, large equivalent stress promoted bone formation and elongated the edges of the dense bone towards the blood vessel. After 100 days, the elongated bone was isolated to form two single trabeculae that aligned along the

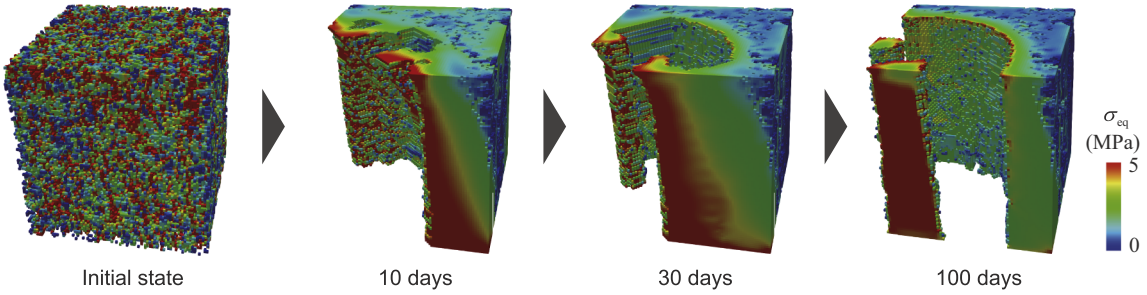

Fig. 3. Reproduction of cortical-like and cancellous-like bone microstructures according to the distance from the blood vessel. The change in two types of bone morphology and the distribution of von Mises equivalent stress for 100 days, under the baseline parameter setting of $S_u/\sigma_0 = 4.0$, $S_l/\sigma_0 = 2.0$, and $\phi_{th}/\phi_0 = 1.0 \times 10^{-2}$, are shown.

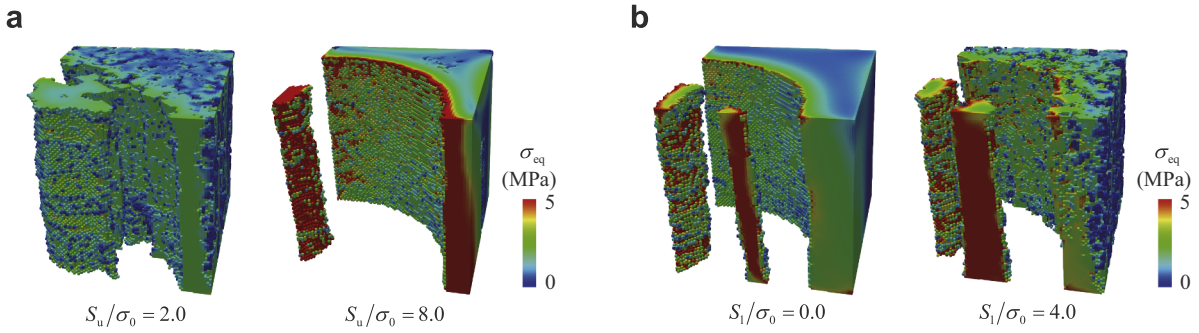

Fig. 4. Bone morphology and the distribution of von Mises equivalent stress after 100-day remodeling. a, Effects of the upper threshold for the mechanical stimulus, S_u. b, Effects of the lower threshold for the mechanical stimulus, S_l.

loading direction. These remodeling processes produced two types of bone with different porosities in the region of analysis: one was a cancellous-like bone composed of multiple trabeculae in the marrow cavity near the blood vessel, and the other was a cortical-like bone surrounding the marrow cavity.

3.2. Effects of the upper and lower thresholds for the mechanical stimulus, S_u and S_l

To show the fundamental characteristics of the proposed remodeling model, we investigated the effects of the upper and lower thresholds for the mechanical stimulus, S_u and S_l, on the cortical-like and cancellous-like bone microstructures. Fig. 4 shows the bone morphology and distribution of von Mises equivalent stress after 100-day remodeling, depending on S_u, where $S_u/\sigma_0 = 2.0$ and 8.0 (Fig. 4a), and S_l, where $S_l/\sigma_0 = 0.0$ and 4.0 (Fig. 4b).

As shown in Fig. 4a, the upper threshold for the mechanical stimulus, S_u, is involved in balancing the bone formation and resorption in the neighborhood of the blood vessel. An increase in S_u promoted bone resorption and reduced local BV/TV near the blood vessel, which resulted in a decrease in the cancellous-like bone volume in the marrow cavity. Furthermore, the loss of bone volume in the marrow cavity enlarged the equivalent stress in the mineralized bone region far from the blood vessel and increased local BV/TV of the cortical-like bone. The lower threshold for the mechanical stimulus, S_l, regulates bone formation in the region far from the blood vessel, as shown in Fig. 4b. In the cortical-like bone region far from the blood vessel, an increase in S_l inhibited bone formation and kept local BV/TV low. However, the increase in S_l had little influence on the cancellous-like bone microstructure close to the blood vessel.

Thus, under a given loading condition, the model parameters S_u and S_l are key regulators of the porosity of cancellous-like and cortical-like bone microstructures, respectively. The gap between S_u and S_l plays an important role in determining the difference between the two types of bone porosities.

3.3. Reproduction of cortical-to-cancellous bone transformation: Effects of the threshold for the molecular concentration, ϕ_{th}

We investigated the effects of the threshold for the molecular concentration, ϕ_{th}, by setting $\phi_{th}/\phi_0 = 1.0$, 1.0×10^{-1}, 1.0×10^{-2} (baseline), 1.0×10^{-3}, and 1.0×10^{-4}. Fig. 5a shows the bone morphology after 100-day remodeling with the distribution of von Mises equivalent stress; Fig. 5b shows the corresponding mean BV/TV in the region at constant distance d away from the blood vessel. The mean BV/TV was quantified in the region defined by $d \pm 0.2$ mm.

In the case of $\phi_{th}/\phi_0 = 1.0$, bone resorption was completely inhibited because the concentration of bone resorption molecules ϕ on the entire bone surface was less than its threshold value ϕ_{th}. Thus, the BV/TV of the bone specimen was increased globally owing to bone formation, which produced a dense bone specimen similar to that of a cortical bone. The decrease in the threshold value ϕ_{th} generated a marrow cavity around the blood vessel ($\phi_{th}/\phi_0 = 1.0 \times 10^{-1}$). With a further decrease in ϕ_{th}, trabeculae were formed in parallel with the loading direction in the enlarged cavity space ($\phi_{th}/\phi_0 = 1.0 \times 10^{-2}$ and 1.0×10^{-3}). Finally, when $\phi_{th}/\phi_0 = 1.0 \times 10^{-4}$, 100-day remodeling produced a porous cancellous-like bone that comprises multiple trabeculae, the structure of which is adapted functionally to the imposed mechanical loading. Thus, the transformation from the dense cortical bone with large BV/TV to the porous cancellous bone with small BV/TV was reproduced successfully.

Collectively, the ratio of the threshold for the molecular concentration ϕ_{th} to the concentration of bone resorption molecules in the blood vessel ϕ_0 is the determinant of the volume ratio between the cortical-like bone and cancellous-like bone. The transformation from cortical to the cancellous bone can be induced by a decrease in ϕ_{th} when ϕ_0 is constant, and further, by an increase in ϕ_0 when ϕ_{th} is constant.

4. Discussion

We propose a novel theoretical concept to account for the transformation of dense cortical bone to porous cancellous bone. Based on the concept that bone porosity is determined by the balance between the load-bearing function of mineralized bone and material-transport function of bone marrow, we developed a mathematical model of cortical and cancellous bone remodeling. The remodeling simulations using this mathematical model enable the reproduction of microstructures of cortical and cancellous bones simultaneously, whereas previous remodeling simulations addressed their remodeling processes separately. Furthermore, the present remodeling simulations have the potential to replicate cortical-to-cancellous bone transformation depending on the change in the local balance between bone formation and resorption.

The validity of the proposed remodeling model was verified qualitatively through comparison of bone microstructures obtained by simulations with those observed in human bone specimens at different ages. As shown in Fig. 5, when the ratio of ϕ_{th} to the molecular concentration in the blood vessel ϕ_0 is relatively high, a small canal, which can be considered as a Haversian canal, was formed around the blood vessel. As the ratio ϕ_{th}/ϕ_0 decreases, the small canal was enlarged, and multiple trabeculae replaced the cortical-like bone. This process is analogous remarkably to the process of age-related cortical bone loss characterized by increase in intracortical porosity and trabecularization of the inner cortex (Bala et al., 2015; Zebaze and Seeman, 2015; Zebaze et al., 2010). For more rigorous model validation, it would be considerably important to compare quantitatively the bone morphometric data obtained by the remodeling simulations with those obtained by corresponding *in vivo* experiments.

The proposed remodeling model includes only three parameters: the upper and lower thresholds for the mechanical stimulus, S_u and S_l, and

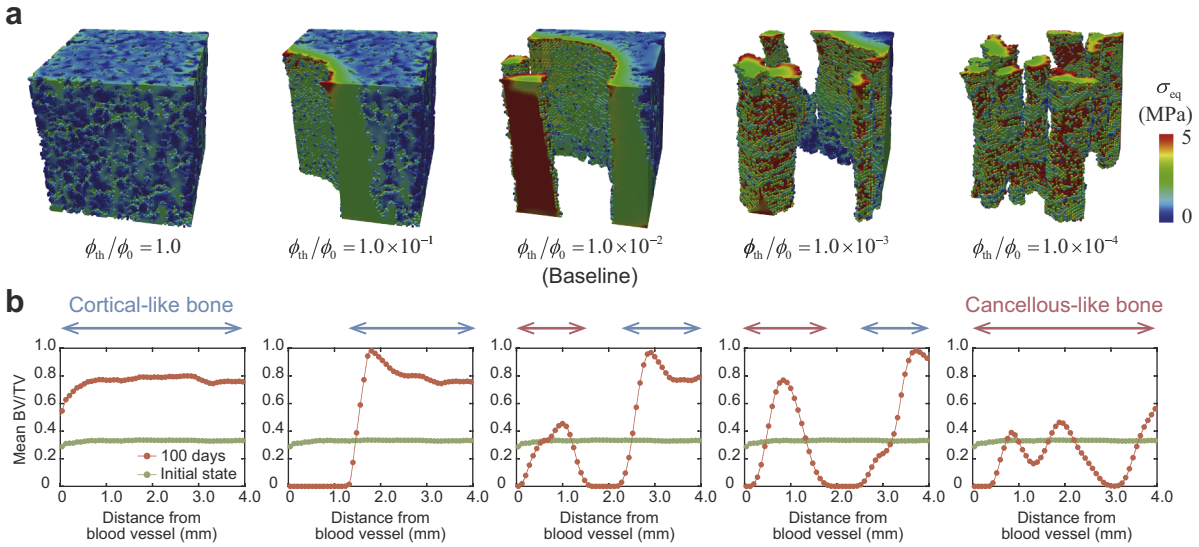

Fig. 5. Reproduction of the transformation from cortical to cancellous bone depending on the threshold for molecular concentration, ϕ_{th}. a, Bone morphology and the distribution of von Mises equivalent stress after 100-day remodeling. b, Distribution of mean bone volume fraction (BV/TV) defined in the region at a constant distance away from the blood vessel.

the threshold for the molecular concentration, ϕ_{th}. S_u and S_l play roles in regulating the porosity of cancellous-like and cortical-like bone, respectively, and ϕ_{th} is an essential parameter governing the volume ratio between the two types of bone, and thus, in the cortical-to-cancellous bone transformation. The model parameter ϕ_{th} can be interpreted as the parameter associated with the sensitivity of effector cells on the bone surface to the bone resorption molecules; the decrease in ϕ_{th} corresponds to the enhancement of sensitivity. Therefore, the simulation results obtained in this study imply that *in vivo* cortical bone loss due to the trabecularization of the cortex can be induced by an increase in the sensitivity of bone surface cells to the bone resorption molecules, *i.e.*, the decrease in ϕ_{th}, and/or increase in the supply of the bone resorption molecules from blood vessels, *i.e.*, an increase in ϕ_0.

Bone remodeling is regulated inherently by a complex signaling cascade that influences many types of cells in mineralized bone and bone marrow (Boyle et al., 2003; Long, 2012), where mechanical and biochemical events are coupled tightly. For reducing such complex cellular and molecular mechanisms of bone remodeling, we assumed that functional balance between mineralized bone and bone marrow determines bone porosity, from a phenomenological viewpoint. Thus, in the proposed modeling, we considered only two determinants—mechanical stimulus as a bone formation factor and hypothetical molecule as a bone resorption factor—to reproduce cortical-to-cancellous bone transformation. Although our phenomenological remodeling model lacks solid biological background, it is valuable for capturing the nature of complex mechano-biochemical coupling phenomena. To clarify the cellular and molecular basis of the cortical-to-cancellous bone transformation, it is necessary to incorporate specific molecular/cellular dynamics and their interrelationship into the mathematical model (Kameo et al., 2020). Despite such limitations, in the future, we anticipate that the proposed mathematical model of cortical and cancellous bone remodeling will contribute to highlight the essential features of the cortical bone loss due to the trabecularization of the cortex and predict its spatial and temporal behavior during aging.

CRediT authorship contribution statement

Yoshitaka Kameo: Conceptualization, Methodology, Software, Writing - Original Draft, Writing - Review & Editing, Funding acquisition. **Nobuaki Sakano**: Software, Validation, Investigation, Visualization. **Taiji Adachi**: Conceptualization, Writing - Original Draft, Supervision, Project administration, Funding acquisition.

Transparency document

The Transparency document associated with this article can be found, in online version.

Declaration of competing interest

None.

Acknowledgments

This study was supported by Grant-in-Aid for Scientific Research (C) (JP19K04074) from Japan Society for the Promotion of Science (JSPS) and by Advanced Research and Development Programs for Medical Innovation (AMED-CREST), Elucidation of Mechanobiological Mechanisms and Their Application to the Development of Innovative Medical Instruments and Technologies (JP19gm0810003) from Japan Agency for Medical Research and Development (AMED).

References

Adachi, T., Tsubota, K., Tomita, Y., Hollister, S.J., 2001. Trabecular surface remodeling simulation for cancellous bone using microstructural voxel finite element models. J. Biomech. Eng. 123, 403–409. https://doi.org/10.1115/1.1392315.

Adachi, T., Aonuma, Y., Taira, K., Hojo, M., Kamioka, H., 2009. Asymmetric intercellular communication between bone cells: propagation of the calcium signaling. Biochem. Biophys. Res. Commun. 389, 495–500. https://doi.org/10.1016/j.bbrc.2009.09.010.

Badilatti, S.D., Christen, P., Levchuk, A., Marangalou, J.H., van Rietbergen, B., Parkinson, I., Muller, R., 2016. Large-scale microstructural simulation of load-adaptive bone remodeling in whole human vertebrae. Biomech. Model. Mechanobiol. 15, 83–95. https://doi.org/10.1007/s10237-015-0715-8.

Bala, Y., Zebaze, R., Seeman, E., 2015. Role of cortical bone in bone fragility. Curr. Opin. Rheumatol. 27, 406–413. https://doi.org/10.1097/bor.0000000000000183.

Bonewald, L.F., 2011. The amazing osteocyte. J. Bone Miner. Res. 26, 229–238. https://doi.org/10.1002/jbmr.320.

Boyle, W.J., Simonet, W.S., Lacey, D.L., 2003. Osteoclast differentiation and activation. Nature 423, 337–342. https://doi.org/10.1038/nature01658.

Gerhard, F.A., Webster, D.J., van Lenthe, G.H., Muller, R., 2009. In silico biology of bone modelling and remodelling: adaptation. Phil. Trans. R. Soc. A 367, 2011–2030. https://doi.org/10.1098/rsta.2008.0297.

Huiskes, R., Ruimerman, R., van Lenthe, G.H., Janssen, J.D., 2000. Effects of mechanical forces on maintenance and adaptation of form in trabecular bone. Nature 405, 704–706. https://doi.org/10.1038/35015116.

Jaworski, Z.F., Lok, E., 1972. The rate of osteoclastic bone erosion in haversian

remodeling sites of adult dogs rib. Calcif. Tissue Res. 10, 103–112. https://doi.org/10.1007/bf02012540.
Kameo, Y., Adachi, T., 2014. Interstitial fluid flow in canaliculi as a mechanical stimulus for cancellous bone remodeling: in silico validation. Biomech. Model. Mechanobiol. 13, 851–860. https://doi.org/10.1007/s10237-013-0539-3.
Kameo, Y., Adachi, T., Hojo, M., 2009. Fluid pressure response in poroelastic materials subjected to cyclic loading. J. Mech. Phys. Solids 57, 1815–1827. https://doi.org/10.1016/j.jmps.2009.08.002.
Kameo, Y., Ootao, Y., Ishihara, M., 2016. Poroelastic analysis of interstitial fluid flow in a single lamellar trabecula subjected to cyclic loading. Biomech. Model. Mechanobiol. 15, 361–370. https://doi.org/10.1007/s10237-015-0693-x.
Kameo, Y., Miya, Y., Hayashi, M., Nakashima, T., Adachi, T., 2020. In silico experiments of bone remodeling explore metabolic diseases and their drug treatment. Sci. Adv. 6, eaax0938. https://doi.org/10.1126/sciadv.aax0938.
Kim, Y.K., Kameo, Y., Tanaka, S., Adachi, T., 2017. Capturing microscopic features of bone remodeling into a macroscopic model based on biological rationales of bone adaptation. Biomech. Model. Mechanobiol. 16, 1697–1708. https://doi.org/10.1007/s10237-017-0914-6.
LeBlanc, A.D., Spector, E.R., Evans, H.J., Sibonga, J.D., 2007. Skeletal responses to space flight and the bed rest analog: a review. J. Musculoskelet. Neuronal Interact. 7, 33–47.
Long, F.X., 2012. Building strong bones: molecular regulation of the osteoblast lineage. Nat. Rev. Mol. Cell Biol. 13, 27–38. https://doi.org/10.1038/nrm3254.
Mendez-Ferrer, S., Michurina, T.V., Ferraro, F., Mazloom, A.R., MacArthur, B.D., Lira, S.A., Scadden, D.T., Ma'ayan, A., Enikolopov, G.N., Frenette, P.S., 2010. Mesenchymal and haematopoietic stem cells form a unique bone marrow niche. Nature 466, 829–U859. https://doi.org/10.1038/nature09262.
Parfitt, A.M., 1994. Osteonal and hemi-osteonal remodeling: the spatial and temporal framework for signal traffic in adult human bone. J. Cell. Biochem. 55, 273–286. https://doi.org/10.1002/jcb.240550303.
Petrtyl, M., Hert, J., Fiala, P., 1996. Spatial organization of the haversian bone in man. J. Biomech. 29, 161–169. https://doi.org/10.1016/0021-9290(94)00035-2.
Ramasamy, S.K., 2017. Structure and functions of blood vessels and vascular niches in bone. Stem Cells Int. https://doi.org/10.1155/2017/5046953.
Robling, A.G., Niziolek, P.J., Baldridge, L.A., Condon, K.W., Allen, M.R., Alam, I., Mantila, S.M., Gluhak-Heinrich, J., Bellido, T.M., Harris, S.E., Turner, C.H., 2008. Mechanical stimulation of bone in vivo reduces osteocyte expression of Sost/sclerostin. J. Biol. Chem. 283, 5866–5875. https://doi.org/10.1074/jbc.M705092200.
Silva, B.C., Bilezikian, J.P., 2015. Parathyroid hormone: anabolic and catabolic actions on the skeleton. Curr. Opin. Pharmacol. 22, 41–50. https://doi.org/10.1016/j.coph.2015.03.005.
Spatz, J.M., Wein, M.N., Gooi, J.H., Qu, Y.L., Garr, J.L., Liu, S., Barry, K.J., Uda, Y., Lai, F., Dedic, C., Balcells-Camps, M., Kronenberg, H.M., Babij, P., Pajevic, P.D., 2015. The Wnt inhibitor sclerostin is up-regulated by mechanical unloading in osteocytes in vitro. J. Biol. Chem. 290, 16744–16758. https://doi.org/10.1074/jbc.M114.628313.
Tsubota, K., Adachi, T., 2004. Changes in the fabric and compliance tensors of cancellous bone due to trabecular surface remodeling, predicted by a digital image-based model. Comput. Methods Biomech. Biomed. Engin. 7, 187–192. https://doi.org/10.1080/10255840410001729524.
van Oers, R.F.M., Ruimerman, R., Tanck, E., Hilbers, P.A.J., Huiskes, R., 2008. A unified theory for osteonal and hemi-osteonal remodeling. Bone 42, 250–259. https://doi.org/10.1016/j.bone.2007.10.009.
Weinbaum, S., Cowin, S.C., Zeng, Y., 1994. A model for the excitation of osteocytes by mechanical loading-induced bone fluid shear stresses. J. Biomech. 27, 339–360. https://doi.org/10.1016/0021-9290(94)90010-8.
Wolff, J., 1870. Ueber die innere Architectur der Knochen und ihre Bedeutung für die Frage vom Knochenwachstum. Virchows Arch. Pathol. Anat. Physiol. Klin. Med. 50, 389–450. https://doi.org/10.1007/bf01944490.
Wolff, J., 2010. The classic on the inner architecture of bones and its importance for bone growth (reprinted from virchows arch pathol anat physiol, vol 50, pg 389–450, 1870). Clin. Orthop. Relat. Res. 468, 1056–1065. https://doi.org/10.1007/s11999-010-1239-2 (2010).
Zebaze, R., Seeman, E., 2015. Cortical bone: a challenging geography. J. Bone Miner. Res. 30, 24–29. https://doi.org/10.1002/jbmr.2419.
Zebaze, R.M.D., Ghasem-Zadeh, A., Bohte, A., Iuliano-Burns, S., Mirams, M., Price, R.I., Mackie, E.J., Seeman, E., 2010. Intracortical remodelling and porosity in the distal radius and post-mortem femurs of women: a cross-sectional study. Lancet 375, 1729–1736. https://doi.org/10.1016/s0140-6736(10)60320-0.
Zebaze, R., Ghasem-Zadeh, A., Mbala, A., Seeman, E., 2013. A new method of segmentation of compact-appearing, transitional and trabecular compartments and quantification of cortical porosity from high resolution peripheral quantitative computed tomographic images. Bone 54, 8–20. https://doi.org/10.1016/j.bone.2013.01.007.